

# 1 JAST (Journal of Animal Science and Technology) TITLE PAGE

Upload this completed form to the website with submission

ARTICLE INFORMATION	Fill in information in each box below
Article Type	Research article
Article Title (within 20 words without abbreviations)	Noninvasive estimation of porcine intramuscular fat from ultrasonography using deep learning
Running Title (within 10 words)	Noninvasive ultrasonographic estimation of porcine intramuscular fat
Author	Tae-kyeong Kim 1#, Young Sin Kim 2#, Soo Hyun Back 2, Joon Ki Hong 3, Jin Soo Kim 4, Hyun-chong Cho 5 #These authors contributed equally to this work.
Affiliation	1 Department of Data Science, Kangwon National University, Chuncheon 24341, Korea 2 Swine Science Division, National Institute of Animal Science, Rural Development Administration, Cheonan 31000, Republic of Korea 3 National Institute of Animal Science Animal Genetics and Breeding Division, National Institute of Animal Science, Rural Development Administration, Cheonan 31000, Republic of Korea 4 Department of Animal Industry Convergence, Kangwon National University, Chuncheon 24341, Korea 5 Department of Electronics Engineering and Department of Data Science, Kangwon National University, Chuncheon 24341, Korea
ORCID (for more information, please visit <a href="https://orcid.org">https://orcid.org</a> )	Tae-kyeong Kim ( <a href="https://orcid.org/0000-0001-8896-416X">https://orcid.org/0000-0001-8896-416X</a> ) Young Sin Kim ( <a href="https://orcid.org/0000-0001-5466-8813">https://orcid.org/0000-0001-5466-8813</a> ) Soo Hyun Back ( <a href="https://orcid.org/0009-0001-2064-4298">https://orcid.org/0009-0001-2064-4298</a> ) Joon Ki Hong ( <a href="https://orcid.org/0000-0001-8272-1263">https://orcid.org/0000-0001-8272-1263</a> ) Jin Soo Kim ( <a href="https://orcid.org/0000-0002-9518-7917">https://orcid.org/0000-0002-9518-7917</a> ) Hyun-chong Cho ( <a href="https://orcid.org/0000-0003-2122-468X">https://orcid.org/0000-0003-2122-468X</a> )
Competing interests	No potential conflict of interest relevant to this article was reported.
Funding sources State funding sources (grants, funding sources, equipment, and supplies). Include name and number of grant if available.	This work was carried out with the support of “Cooperative Research Program for Agriculture Science and Technology Development (Project No. PJ012636)” Rural Development Administration, Korea
Acknowledgements	This work was carried out with the support of the “Study on improvement of economic traits and industry vitalization of chookjin breeding pig (Project No. PJ012636)” Rural Development Administration, Korea and this work was supported by Korea Institute of Planning and Evaluation for Technology in Food, Agriculture and Forestry (IPET) and Korea Smart Farm R&D Foundation (KosFarm) through Smart Farm Innovation Technology Development Program, funded by Ministry of Agriculture, Food and Rural Affairs (MAFRA) and Ministry of Science and ICT (MSIT), Rural Development Administration (RDA) (2540001233) and this research was supported by the Basic Science Research Program through the National Research Foundation of Korea (NRF) funded by the Ministry of Education (No. 2022R111A3053872) and the National Research Foundation of Korea (NRF) grant funded by the Korea government (MSIT) (RS-2023-00242528).
Availability of data and material	Upon reasonable request, the datasets of this study are available from the corresponding author.
Authors’ contributions Please specify the authors’ role using this form.	Conceptualization: HCC, JSK, YSK, JKH Data curation: JSK, SHB Formal analysis: HCC Methodology: TKK, HCC, YSK, JKH Software: TKK, HCC Validation: JSK, HCC, YSK, JKH Investigation: TKK, HCC, SHB Writing - original draft: TKK, JSK, HCC, YSK, SHB, JKH
Ethics approval and consent to participate	This study was approved by IACUC of Rural Development Administration (No. NIAS2020-0478), Korea.

2

## CORRESPONDING AUTHOR CONTACT INFORMATION

For the corresponding author (responsible for correspondence, proofreading, and reprints)	Fill in information in each box below
First name, middle initial, last name	Jin Soo Kim // Hyun-chong Cho
Email address – this is where your proofs will be sent	kjs896@kangwon.ac.kr // hyuncho@kangwon.ac.kr
Secondary Email address	

Address	Department of Animal Industry Convergence, Kangwon National University, Chuncheon 24341, Korea // Department of Electronics Engineering and Department of Data Science, Kangwon National University, Chuncheon 24341, Korea
Cell phone number	+82-10-2566-5961 // +82-10-5775-8370
Office phone number	+82-33-250-8614 // +82-33-250-6301
Fax number	+82-33-259-5572 // +82-33-259-5674

### Abstract

Intramuscular fat (IMF) is a principal determinant of pork loin quality and a critical factor in meat grading and consumer preference. This study proposes a Transformer-based deep learning framework for noninvasive quantitative estimation of porcine IMF from B-mode ultrasonographic images. A total of 9,409 single-channel ultrasound frames were acquired using a 3.5-MHz system targeting the *longissimus thoracis et lumborum* and subcostal regions. The dataset comprised 3,949 pigs, including 47 animals with directly measured IMF values and 3,902 animals with IMF estimates generated by the Biosoft ultrasound analysis program. To address the limited availability of measured ground-truth data, we adopted a Vision Transformer–Huge (ViT-H) regression model and incorporated a teacher–student knowledge distillation strategy. The teacher model was trained using large-scale Biosoft-derived IMF estimates, and the student model was trained using measured IMF values while simultaneously learning from the teacher’s soft predictions. An uncertainty-aware distillation loss was introduced to adaptively weight the distillation signal based on the teacher model’s predictive variance, thereby mitigating the transfer of unreliable knowledge. In addition, RandAugment was applied during training to enhance generalization under limited data conditions. Model performance was evaluated using mean absolute percentage error (MAPE) with five-fold cross-validation. Compared with the conventional Biosoft-based regression baseline (MAPE: 43.61%), the ViT-H regression model substantially reduced prediction error (34.78%). Incorporating knowledge distillation further improved performance (34.361%), and uncertainty-aware distillation yielded additional gains (33.859%). The best performance was achieved by combining uncertainty-aware distillation with RandAugment, yielding a MAPE of 31.313%. These findings demonstrate that Transformer-based regression combined with uncertainty-aware knowledge distillation provides a robust and scalable solution for IMF estimation from ultrasound images and may help distinguish IMF differences relevant to commercial pork quality grading, although further validation is required. The proposed framework effectively leverages both limited measured data and large-scale predicted data, enabling accurate, practical, and noninvasive IMF assessment suitable for on-farm and near-real-time applications in precision livestock production.

**Keywords:** Deep learning; meat quality; noninvasive estimation; porcine intramuscular fat; ultrasonography

29

30

## Introduction

31 Pork is the most widely consumed meat in South Korea [1], and meat quality is a primary determinant of  
32 consumer purchasing decisions [2]. Within the Korean livestock product grading system, intramuscular fat (IMF)  
33 content is one of several factors considered in determining pork quality grade [3]. It is considered alongside other  
34 critical attributes, such as fat thickness, meat color, and texture, because it is closely linked to palatability. In  
35 particular, higher IMF levels are associated with improved tenderness, juiciness, and flavor, which in turn shape  
36 consumer satisfaction and their willingness to purchase. Accordingly, a reliable and practical IMF assessment is  
37 essential, not only for producers seeking to align products with market expectations but also for sustaining  
38 competitiveness throughout the supply chain. These considerations have motivated the development of methods  
39 that can accurately and consistently quantify the IMF at low operational cost, thereby supporting quality-focused  
40 decision-making from the point of production to retail outlets. In commercial settings, methods that minimize  
41 invasiveness, such as noninvasive imaging techniques, and reduce turnaround time are particularly desirable.

42 Despite their utility in grading and research, the prevailing methods for IMF estimation face practical,  
43 methodological, and ethical constraints. Carcass-based chemical analyses provide reference values but are  
44 inherently postmortem, preventing assessment during the rearing process and increasing the turnaround time and  
45 cost; consequently, such analyses cannot support longitudinal management decisions at the farm level. They also  
46 rely on destructive sampling of specific muscles, for example, the *longissimus thoracis et lumborum* and, by  
47 definition, yield a single cross-section per carcass, offering no opportunity for repeated measurements in the same  
48 animal. The inability to obtain IMF estimates during the rearing process remains a major operational barrier for  
49 producers seeking to stratify animals before shipment, adjust feeding regimes, or evaluate genetic lines *in vivo*.

50 To enable live animal assessment of IMF, three main approaches have been investigated: biopsy-based  
51 sampling [4], CT imaging [6], and ultrasonography (US) [7].

52 In a large-scale study of 216 pigs (732 samples), Bosch et al. [4] showed that the sampling strategy  
53 significantly affected IMF and fatty acid (FA) estimates. Biopsies from live animals tended to overestimate  
54 IMF and polyunsaturated FA, while smaller samples underestimated monounsaturated FA, indicating  
55 systematic sampling bias. Although analytically reliable, biopsy methods are invasive and raise welfare and  
56 productivity concerns [5], limiting their suitability for repeated or large-scale on-farm use.

57 CT imaging has been evaluated as a noninvasive alternative in 104 pigs [6], where IMF was predicted from  
58 filtered CT images using partial least squares regression. Despite its technical feasibility, CT requires ionizing  
59 radiation, expensive, immobile equipment, and specialized facilities, limiting its scalability in commercial  
60 settings.

61 Ultrasound provides a portable and radiation-free option. In a study of 574 pigs [7], IMF was estimated from  
62 segmented B-mode images using mean grayscale intensity, achieving RMSE of 0.54% and  $R^2$  of 0.56. However,  
63 there was no clear explanation regarding external validation or data splitting, and the model was trained and  
64 evaluated on the same dataset. The reference values for backfat and loin depth were not based on actual carcass  
65 measurements, but rather on readings from another ultrasound-based semi-automated software called Biosoft.  
66 Additionally, the IMF estimation model had a strong breed effect, so a significant portion of the IMF variance  
67 may have been explained by breed differences. This suggests that the model may have predicted the average  
68 IMF level based on breed information rather than learning subtle tissue signals from ultrasound images.

69 Collectively, prior work demonstrates that biopsy is accurate but invasive, CT is noninvasive but impractical  
70 for routine use, and ultrasound is deployable yet constrained by feature engineering. A remaining gap is the  
71 need for a portable, noninvasive framework that leverages learning-based models to capture multiscale image  
72 patterns directly from data. The present study addresses this limitation.

73 US images can be inherently challenging to analyze because of speckle noise, heterogeneous tissue  
74 echogenicity, and anatomical variability, underscoring the need for more sophisticated techniques. Consequently,  
75 advanced computational methods—most notably deep learning models—have been actively explored to improve  
76 the accuracy and reliability of IMF estimation. Accordingly, deep-learning-based computer-aided diagnosis  
77 (CADx) for US has gained momentum in diverse clinical applications [8]. By learning task-specific  
78 representations directly from data, deep models can automatically extract features relevant to IMF, capture  
79 complex spatial patterns, and deliver rapid inference, which is beneficial for large cohorts and near-real-time use.  
80 These properties also support scalability and adaptation to industrial settings with a focus on pork quality  
81 assessments. A recent study used data from 945 commercial pigs to estimate the IMF [9]. The proposed prediction  
82 of intramuscular fat percentage (PIMFP) model converted images to grayscale, selected regions of interest,  
83 applied contrast enhancement, and then trained a ResNet-50-based deep neural network to output the IMF. An  
84 RMSE of 0.59% was reported, demonstrating the feasibility of deep-learning models for IMF estimation from US.  
85 Moreover, the reliance on predefined preprocessing (grayscale conversion, ROI selection, and contrast heuristics)

86 highlights the opportunity for an end-to-end methodology that jointly learns representations and predictions,  
87 potentially improving the model's robustness across operators and acquisition settings.

88 Prior IMF estimation methods balance accuracy, practicality, and noninvasiveness. Carcass chemistry and  
89 biopsies provide reference values but are invasive and unsuitable for longitudinal use, while CT offers improved  
90 imaging yet is costly, nonportable, and uses ionizing radiation. Accordingly, recent studies have explored  
91 ultrasonography with deep learning, though comprehensive evaluations remain limited. In actual farm  
92 environments, precise IMF measurements are limited by cost and procedural constraints, making it difficult to  
93 secure sufficiently accurate data. These data shortages have acted as structural limitations to improving the  
94 performance of ultrasound-based IMF estimation models. Research that achieves high regression performance  
95 using limited measurement data is relatively rare.

96 In this study, we proposed a method for quantitatively estimating intramuscular fat using B-mode ultrasound  
97 data. We developed a knowledge distillation-based model to complement limited measured data by utilizing soft  
98 labels generated by Biosoft, a previously developed ultrasound-based intramuscular fat estimation program [10].  
99 We also introduced an uncertainty-aware knowledge distillation loss to reflect prediction uncertainty, thereby  
100 improving model performance. To address the issue of insufficient measured data, we further applied  
101 RandAugment. The main performance evaluation metric was mean absolute percentage error (MAPE), which is  
102 intuitively interpretable in livestock farming settings. We ultimately achieved an MAPE of approximately  
103 31.313%.

104 Our objective was to identify an accurate, practical, and noninvasive method suitable for on-farm, near-real-  
105 time monitoring of IMF during the rearing process. Such capabilities could support quality-focused management  
106 and selection, improve process efficiency across the production chain, and enhance consumer satisfaction and  
107 market competitiveness.

108

## 109 **Materials and Methods**

### 110 **Dataset**

111 The study was approved by the IACUC of the Rural Development Administration, Korea (Approval No.  
112 NIAS2020-0478), and the dataset used in this study was provided by the Research Department at the National  
113 Institute of Animal Science in Cheonan-si, Chungnam, South Korea. The data used in this study were collected  
114 from 3,949 pigs (including Duroc and Woori Heukdon breeds). Among them, 47 pigs were slaughtered to obtain  
115 direct measurements of intramuscular fat (IMF). For the remaining 3,902 pigs, IMF values were estimated using

116 the ultrasound image analysis software, Biosoft [10]. For each pig, one to three ultrasound images were collected.  
117 All splits used for five-fold cross-validation were performed at the individual ID level, ensuring that images from  
118 the same pig were included in only one fold. Further details are provided in Table 1.

119 The images were acquired using the Exago US system (IMV Imaging) operating at 3.5 MHz, with a depth of  
120 140 mm and a focal length of 60 mm [11]. The target acquisition sites were the *longissimus thoracis et lumborum*  
121 and subcostal region (beneath the last rib), both of which are commonly used to evaluate the IMF. Representative  
122 raw frames are shown in Figure 1.

### 123 **Deep-learning-based regression models for IMF estimation**

124 This study aimed to quantitatively estimate the IMF in B-mode US images using supervised regression.  
125 Conventional image classification models assign images to predefined categories, which can be useful for learning  
126 generic visual patterns; however, they are suboptimal for predicting continuous targets. Accordingly, we adapted  
127 the classification backbones by replacing the final classification head with a single-output regression head to  
128 predict the IMF as a continuous value. This modification enabled end-to-end training on pixel-level textures and  
129 anatomical cues that correlated with the IMF, yielding precise quantitative estimates under regression loss.

130 We adopted a Transformer-based architecture for IMF estimation from ultrasound (US) images, specifically  
131 utilizing the ViT-H (Vision Transformer Huge) model. To match the model's input requirements, single-channel  
132 B-mode US frames were replicated across three channels. The ViT-H model tokenizes an image into fixed-size  
133 patches and leverages self-attention mechanisms to capture long-range dependencies across the entire spatial  
134 domain [12]. This global attention enables the model to integrate contextual information from distant regions  
135 within the image, which is particularly beneficial for understanding distributed texture patterns and morphological  
136 variations in US data. Such characteristics are crucial in the context of intramuscular fat estimation, where subtle  
137 and spatially distributed visual cues can influence prediction accuracy. By leveraging the Transformer  
138 architecture's global receptive field and data-driven inductive bias, the model effectively learns complex visual  
139 patterns associated with IMF. Model performance was evaluated using MAPE under standardized experimental  
140 conditions.

141

### 142 **Knowledge Distillation-Based Teacher-Student Learning**

143 In this study, we applied the teacher-student-based knowledge distillation [13]. Knowledge distillation transfers  
144 predictive information from a pretrained teacher model to a student model, encouraging the student to learn  
145 representations with improved generalization.

146 The teacher model was trained using only intramuscular fat data derived from Biosoft values. The teacher  
147 model was sufficiently trained using this IMF information, and its weights were fixed during the subsequent  
148 student training stage.

149 The student model was trained using measured data collected in real field conditions as input. During student  
150 training, two types of losses were applied simultaneously. First, a supervised loss was computed using the  
151 measured values as ground truth. Second, a distillation loss was introduced to minimize the discrepancy between  
152 the teacher and student models' predictions for the same input. The distillation loss was calculated as the error  
153 between the teacher and student predictions. The final loss was defined as a linear combination of the supervised  
154 and distillation losses, with their respective weighting factors. Through this training strategy, the student model  
155 was designed to reflect not only the direct supervision from measured data but also the predictive tendencies of  
156 the teacher model trained on Biosoft-based IMF information. Consequently, the student model preserves the  
157 characteristics of the measured data while indirectly absorbing knowledge transferred from reliable IMF-based  
158 information.

159 Also, because the available training data were limited, K-fold cross-validation was used to enhance the  
160 robustness of the student model. In this study, a 5-fold cross-validation strategy was adopted, dividing the dataset  
161 into 5 mutually exclusive subsets. For each iteration, four subsets were used for training, and the remaining subset  
162 was used for validation. This process was repeated five times so that each subset served as the validation set once.

### 163 **Uncertainty-Aware Knowledge Distillation**

164 In addition to the standard knowledge distillation framework, we further introduce an uncertainty-aware  
165 distillation strategy to improve training stability and predictive accuracy [14]. In conventional knowledge  
166 distillation, the distillation loss is applied uniformly to all samples, regardless of the reliability of the teacher's  
167 predictions. However, when the teacher model exhibits high uncertainty for certain samples, enforcing strong  
168 distillation on those samples may transfer unreliable knowledge to the student model, thereby degrading  
169 performance. To address this issue, we estimate the teacher model's predictive uncertainty via dropout during  
170 inference. Specifically, eight stochastic forward passes are performed with dropout activated, and the variance of  
171 the teacher predictions is computed as a measure of uncertainty.

172 Samples with higher predictive variance are considered more uncertain. Based on this uncertainty estimate, the  
173 distillation loss contribution is adaptively adjusted for each sample. When the teacher's uncertainty is high, the  
174 weight assigned to the distillation loss is reduced, thereby weakening the influence of unreliable teacher  
175 predictions. Conversely, when the teacher's uncertainty is low, the distillation loss is emphasized to effectively

176 transfer reliable knowledge. The final training objective is formulated as a weighted combination of the supervised  
177 loss and the uncertainty-modulated distillation loss. This uncertainty-aware knowledge distillation strategy allows  
178 the student model to selectively learn from confident teacher predictions while relying more on ground truth  
179 supervision for ambiguous samples. As a result, compared with fixed weight distillation, the proposed method  
180 provides more stable optimization and achieves improved prediction accuracy.

### 181 **RandAugment Augmentation Method**

182 Finally, we applied RandAugment only during training as a data augmentation strategy [15]. RandAugment is  
183 a simplified automatic data augmentation method that randomly selects a fixed number of augmentation  
184 operations from a predefined set (e.g., rotation, translation, color adjustment, shear) and applies them with a  
185 uniformly controlled magnitude. Unlike earlier policy-search-based approaches such as AutoAugment,  
186 RandAugment eliminates the need for computationally expensive searches over augmentation policies by using  
187 only two hyperparameters: the number of transformations (N) and the magnitude (M). This design enables  
188 efficient and scalable augmentation while maintaining strong performance. In this study, N and M were set to 2  
189 and 9, respectively.

190 RandAugment provides diverse and effective transformations without requiring an extensive search for optimal  
191 augmentation policies, thereby improving generalization performance. It enhances robustness by exposing the  
192 model to a wide range of appearance variations. In this study, we applied RandAugment specifically because the  
193 amount of measured data were limited. By artificially increasing data diversity through random transformations,  
194 we aimed to compensate for the insufficient number of measured samples and to mitigate overfitting caused by  
195 the scarcity of training data. The overall research flow chart is shown in Figure 2.

196 The experiments were executed on an Intel Core i9-10920X CPU running at 3.50 GHz with an NVIDIA  
197 GeForce RTX 3090 and 64 GB RAM using Python 3.11.7, PyTorch 2.1.2, and CUDA 12.1. All training ran for  
198 100 epochs with a batch size of eight using the Adam optimizer (learning rate 0.0001). Early stopping was  
199 triggered when the validation loss plateaued to mitigate overfitting.

200

## 201 **Results and Discussion**

### 202 **Quantitative performance metrics**

203 In this study, the predictive performance of the ultrasonographic IMF regression model was evaluated using  
204 the mean absolute percentage error (MAPE). MAPE is defined as the mean of the absolute percentage differences  
205 between predicted and reference values and quantifies model error on a relative scale. Unlike scale-dependent

206 metrics, MAPE expresses deviations as percentages of the true values, enabling direct interpretability and  
207 facilitating comparison across experimental conditions. This property is particularly relevant for IMF estimation,  
208 where relative prediction error is often more meaningful for production decisions than absolute error magnitude.  
209 Moreover, MAPE provides a balanced and robust summary of prediction performance without  
210 disproportionately amplifying large deviations, thereby offering a stable estimate of generalization performance  
211 in practical settings.

### 212 **Baseline Model results**

213 As described in the Materials and Methods section, the mean absolute percentage error was calculated for 47  
214 animals for which both the predicted values generated by Biosoft and the corresponding measured values were  
215 available. The mean absolute percentage error of the conventional Biosoft-based prediction model was 43.61%,  
216 which was defined as the baseline in this study. For the same 47 animals, the ViT-H model was applied, and K-  
217 fold cross-validation was performed, resulting in a mean absolute percentage error of 34.78%. This result indicates  
218 a substantial reduction in prediction error compared with the baseline.

219 The conventional Biosoft system selects eight texture variables using stepwise regression and constructs a  
220 multiple linear regression model, which relies on predefined variable combinations and linear assumptions. In  
221 contrast, the ViT-H model automatically extracts high-dimensional image features via a Vision Transformer  
222 architecture and learns both global contextual information and local patterns simultaneously. In addition, it  
223 directly models nonlinear relationships, enabling more effective representation of complex tissue structures and  
224 interactions among pixels. These structural differences are interpreted as contributing to improved predictive  
225 performance compared with the traditional regression approach that depends on variable selection.

226 Overall, the ViT-H model reduced prediction error relative to the conventional method and demonstrated more  
227 stable, consistent performance across the dataset. Although a mean absolute percentage error of 34.78% still  
228 indicates a discrepancy between predicted and actual values, this study's results suggest that a transformer-based  
229 deep learning approach has the potential to replace or complement conventional statistical models for estimating  
230 intramuscular fat in pigs.

### 231 **Knowledge Distillation-Based Model results**

232 Additional experiments were conducted using Knowledge Distillation on the ViT-H model. The model with  
233 Knowledge Distillation achieved a MAPE of 34.361%, representing a reduction of 0.419 percentage points  
234 compared to the baseline model without Knowledge Distillation, which recorded 34.78%. This result

235 demonstrates that, under identical training data conditions, the Knowledge Distillation strategy further reduced  
236 prediction error.

237 Through Knowledge Distillation, the student model learned the teacher model's continuous prediction  
238 distribution, enabling it to exploit richer representational information beyond simple regression to ground-truth  
239 values. This study utilized not only 47 samples with measured values but also large-scale prediction data generated  
240 by Biosoft as auxiliary supervision signals. As a result, the approach alleviated the issue of limited information  
241 arising from the constrained measured dataset and more effectively captured the distributional characteristics and  
242 latent patterns of intramuscular fat.

243 This semi-supervised learning framework is highly practical, as it enables the use of accumulated prediction  
244 data from existing systems even when obtaining measured data is challenging. Furthermore, the model with  
245 Knowledge Distillation consistently reduced error compared to the baseline, indicating that the proposed training  
246 strategy further improved the model's generalization performance.

#### 247 **Uncertainty-Aware Knowledge Distillation-Based Model Results**

248 Next, we describe the performance evaluation results of the proposed Uncertainty-aware Knowledge  
249 Distillation method. The proposed method is designed to effectively distill reliable knowledge into the student  
250 model by accounting for the teacher model's predictive uncertainty. When conventional Knowledge Distillation  
251 was applied, the MAPE was 34.361%, whereas the proposed uncertainty-aware method achieved 33.859%,  
252 resulting in an improvement of 0.502 percentage points.

253 Although the absolute difference may appear marginal, its significance extends beyond a simple improvement  
254 in accuracy. The proposed method reduces reliance on unreliable soft targets and mitigates error propagation  
255 during training. These results demonstrate that properly leveraging uncertainty information can address the  
256 limitations of conventional knowledge distillation methods and enable the training of a more stable and  
257 generalized student model. Consequently, the proposed method is experimentally validated as an effective  
258 approach that improves both the reliability and efficiency of the knowledge distillation process.

#### 259 **Proposed Model results**

260 Finally, we describe the results obtained by applying RandAugment to the uncertainty-based knowledge  
261 distillation framework during training. RandAugment was used only during training, and the resulting model  
262 achieved a Mean Absolute Percentage Error of 31.313%. Compared with the best performance from the previous  
263 experiment (33.859%), this represents an improvement of approximately 2.546 percentage points, the best result  
264 among all proposed methods in this study.

265 The performance gain can be attributed to the student model's enhanced generalization, enabled by  
266 RandAugment, which exposed it to a broader range of input distributions. In particular, because the soft targets  
267 from the teacher model had already been adjusted to incorporate uncertainty information, the additional data  
268 diversity likely enabled the student model to learn more robustly under uncertain prediction scenarios. In other  
269 words, the uncertainty-controlled distillation signals and the increased input diversity acted in a complementary  
270 manner, contributing to improved predictive accuracy. Furthermore, given the inherently speckle-rich nature of  
271 ultrasound imaging, the augmentation policies also improve robustness against noise-related variations. By  
272 exposing the student model to intensity perturbations, contrast variations, and geometric transformations,  
273 RandAugment implicitly simulates fluctuations in speckle patterns and acquisition-dependent noise  
274 characteristics. This encourages the model to focus on anatomically meaningful structural cues rather than  
275 overfitting stochastic speckle artifacts, thereby enhancing noise tolerance and stability under real-world ultrasound  
276 conditions. The overall performance of this study is shown in Table 2.

277 These findings also provide important practical implications. In precision analysis tasks such as intramuscular  
278 fat prediction in pigs, which is a primary application of this study, model generalization is a critical factor that  
279 determines real-world applicability. With improved predictive accuracy, we can more precisely estimate  
280 individual quality prior to slaughter, thereby enhancing decision-making in meat grading, feed efficiency  
281 management, and genetic selection. Therefore, the results demonstrate that the proposed method not only  
282 improves performance but also achieves a level of reliability and practicality suitable for real livestock production  
283 environments.

## 284 **Conclusions**

285 This study proposed a Transformer-based regression framework for IMF estimation in B-mode ultrasound  
286 images of pigs and systematically enhanced its performance through knowledge distillation, uncertainty-aware  
287 distillation, and data augmentation. Compared with the conventional Biosoft-based regression approach, the ViT-  
288 H model substantially reduced the mean absolute percentage error, demonstrating the effectiveness of deep  
289 learning-based feature extraction and nonlinear modeling for IMF prediction.

290 The teacher-student knowledge distillation framework enabled the student model to leverage large-scale IMF  
291 prediction data derived from Biosoft, thereby alleviating the limitations imposed by the small number of measured  
292 samples. Incorporating predictive uncertainty into the distillation process further improved training stability by  
293 selectively transferring reliable knowledge from the teacher model. The addition of RandAugment significantly  
294 enhanced generalization performance, yielding the best predictive accuracy among all evaluated configurations.

295 Nevertheless, this study has important limitations. All ultrasound data were acquired under a single acquisition  
296 environment, including a fixed device, imaging parameters, and protocol. Although this controlled setting ensured  
297 experimental consistency, it restricts the external validity of the model. In real-world livestock production,  
298 variations in ultrasound systems, operators, and farm conditions may introduce domain shifts that were not  
299 explicitly addressed in this study. Furthermore, the number of samples with directly measured IMF values was  
300 limited, which may constrain the model's ability to fully capture biological variability despite the use of  
301 knowledge distillation.

302 Future research should therefore focus on validating the proposed framework across multi-center datasets  
303 collected under heterogeneous acquisition conditions. Incorporating domain adaptation or domain generalization  
304 techniques may improve robustness against distribution shifts. Expanding the number of directly measured IMF  
305 samples would further strengthen model reliability. Additionally, integrating multimodal information and  
306 exploring lightweight or compressed model architectures could facilitate practical deployment in on-farm  
307 environments.

308 Overall, the proposed uncertainty-aware knowledge distillation framework combined with Transformer-based  
309 regression provides a promising approach for quantitative IMF estimation from ultrasound images. Compared  
310 with conventional statistical models that rely on predefined variables and linear assumptions, the proposed  
311 approach leverages global contextual modeling, nonlinear representation learning, uncertainty-guided knowledge  
312 transfer, and data-driven augmentation within a unified framework. While the proposed method improved MAPE  
313 relative to the Biosoft-based regression baseline in this study, further validation on multi-environment datasets  
314 with more directly measured IMF samples is required to confirm robustness before routine large-scale deployment.

315

316

## Acknowledgments

317 This work was carried out with the support of the “Study on improvement of economic traits and  
318 industry vitalization of chookjin breeding pig (Project No. PJ012636)” Rural Development  
319 Administration, Korea and this work was supported by Korea Institute of Planning and Evaluation for  
320 Technology in Food, Agriculture and Forestry (IPET) and Korea Smart Farm R&D Foundation  
321 (KosFarm) through Smart Farm Innovation Technology Development Program, funded by Ministry of  
322 Agriculture, Food and Rural Affairs (MAFRA) and Ministry of Science and ICT (MSIT), Rural  
323 Development Administration (RDA) (2540001233) and this research was supported by the Basic  
324 Science Research Program through the National Research Foundation of Korea (NRF) funded by the

325 Ministry of Education (No. 2022R1I1A3053872) and the National Research Foundation of Korea (NRF)  
326 grant funded by the Korea government (MSIT) (RS-2023-00242528).

327

328

## Competing Interests

329 No potential conflict of interest relevant to this article was reported.

330

## Author's Contributions

331 Conceptualization: HCC, JSK, YSK, JKH

332 Data curation: JSK, SHB

333 Formal analysis: HCC

334 Methodology: TKK, HCC, YSK, JKH

335 Software: TKK, HCC

336 Validation: JSK, HCC, YSK, JKH

337 Investigation: TKK, HCC, SHB

338 Writing - original draft: TKK, JSK, HCC, YSK, SHB, JKH

339

340

## Ethics Approval and Consent to Participate

341 This study was approved by IACUC of Rural Development Administration (No. NIAS2020-0478),  
342 Korea.

343

344

345

## References

346 [1] Korea Agricultural Statistics Service. Meat consumption by country (Beef), Meat consumption by country  
347 (Pork); 2022; Meat consumption by country, Chicken.

348 [https://kass.mafra.go.kr/statHtml/statHtml.do?orgId=114&tblId=DT\\_114931\\_HD0100&conn\\_path=I2](https://kass.mafra.go.kr/statHtml/statHtml.do?orgId=114&tblId=DT_114931_HD0100&conn_path=I2),

349 [https://kass.mafra.go.kr/statHtml/statHtml.do?orgId=114&tblId=DT\\_114931\\_HD0200&conn\\_path=I2](https://kass.mafra.go.kr/statHtml/statHtml.do?orgId=114&tblId=DT_114931_HD0200&conn_path=I2),

350 [https://kass.mafra.go.kr/statHtml/statHtml.do?orgId=114&tblId=DT\\_114931\\_HD0300&conn\\_path=I2](https://kass.mafra.go.kr/statHtml/statHtml.do?orgId=114&tblId=DT_114931_HD0300&conn_path=I2)

351 [2] National Institute of Animal Science. Pork Consumption Status and Consumer Perception and Attitudes. 2015.

352 <https://www.nias.go.kr/front/prboardView.do?cmCode=M090814150936066&boardSeqNum=278>

353 [3] Ministry of Agriculture, Food and Rural Affairs. [Detailed standards for grading livestock products]. 2018.11.

354 <https://www.mafra.go.kr/home/5097/subview.do?enc=Zm5jdDF8QEB8JTJGYmJzJTJGaG9tZSUyRjc4OCUyRjQ3NTM3MCUyRmFydGNsVmllldy5kbyUzRg%3D%3D>

355 <https://www.mafra.go.kr/home/5097/subview.do?enc=Zm5jdDF8QEB8JTJGYmJzJTJGaG9tZSUyRjc4OCUyRjQ3NTM3MCUyRmFydGNsVmllldy5kbyUzRg%3D%3D>

356 [4] Bosch L, Tor M, Reixach J, Estany J. Estimating intramuscular fat content and fatty acid composition in live

357 and post-mortem samples in pigs. *Meat Sci.* 2009;82(4):432-437. <https://doi.org/10.1016/j.meatsci.2009.02.013>

- 358 [5] Martínez-Miró S, Tecles F, Ramón M, Escribano D, Hernández F, Madrid J, et al. Causes, consequences and  
359 biomarkers of stress in swine: an update. *BMC Vet Res.* 2016;12:1-9. [https://doi.org/10.1186/s12917-016-0791-](https://doi.org/10.1186/s12917-016-0791-8)  
360 8
- 361 [6] Kongsro J, Gjerlaug-Enger E. In vivo prediction of intramuscular fat in pigs using computed tomography.  
362 *Open J Anim Sci.* 2013;3(4):321. <https://doi.org/10.4236/ojas.2013.34048>
- 363 [7] Peppmeier ZC, Howard JT, Knauer MT, Leonard SM. Estimating backfat depth, loin depth, and intramuscular  
364 fat percentage from ultrasound images in swine. *Anim.* 2023;17(10):100969.  
365 <https://doi.org/10.1016/j.animal.2023.100969>
- 366 [8] Aggarwal R, Sounderajah V, Martin G, Ting DS, Karthikesalingam A, King D. Diagnostic accuracy of deep  
367 learning in medical imaging: a systematic review and meta-analysis. *NPJ Digit. Med.* 2021;4(1):65.  
368 <https://doi.org/10.1038/s41746-021-00438-z>
- 369 [9] Liu Z, Du H, Lao FD, Shen ZC, Lv YH, Zhou L. PIMFP: An accurate tool for the prediction of intramuscular  
370 fat percentage in live pigs using ultrasound images based on deep learning. *Comput. Electron. Agri.*  
371 2024;217:108552
- 372 [10] Biotronics, Inc. (2025). BioSoft Toolbox software for live animal ultrasound measurement and carcass trait  
373 prediction. Retrieved from <https://www.biotronics-inc.com/live-animal-software>
- 374 [11] IMV Imaging, ExaGo portable ultrasound scanner: [https://www.imv-imaging.com/world/support/exago-](https://www.imv-imaging.com/world/support/exago-ultrasound-product-support)  
375 [ultrasound-product-support](https://www.imv-imaging.com/world/support/exago-ultrasound-product-support). 2025.
- 376 [12] Dosovitskiy A, Beyer L, Kolesnikov A, Weissenborn D, Zhai X, Unterthiner T. An image is worth 16x16  
377 words: Transformers for image recognition at scale. arXiv preprint arXiv: 2020.11929.
- 378 [13] Hinton, G., Vinyals, O., & Dean, J. (2015). Distilling the knowledge in a neural network. *arXiv preprint*  
379 *arXiv:1503.02531*.
- 380 [14] Yang, Y., Wang, C., Gong, L., Wu, M., Chen, Z., Gao, Y., ... & Zhou, X. (2024). Uncertainty-Aware Self-  
381 Knowledge Distillation. *IEEE Transactions on Circuits and Systems for Video Technology*.
- 382 [15] Cubuk, E. D., Zoph, B., Shlens, J., & Le, Q. V. (2020). RandAugment: Practical automated data augmentation  
383 with a reduced search space. In *Proceedings of the IEEE/CVF conference on computer vision and pattern*  
384 *recognition workshops* (pp. 702-703).
- 385

386

**Tables**387 **Table 1.** Detail of dataset

<b>Dataset Type</b>	<b>Number of pigs</b>	<b>Number of images</b>	<b>Mean and standard deviation of intramuscular fat</b>
<b>Biosoft</b>	3,902	9,329	2.966±0.919
<b>Actual measurement</b>	47	80	3.233±1.472

388

ACCEPTED

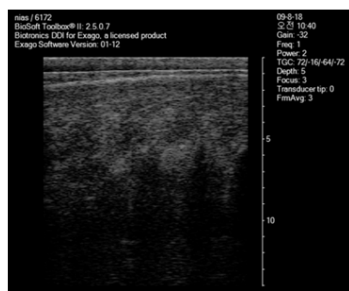
389 **Table 2.** The overall performance of this study

<b>Method</b>	<b>Mean Absolute Percentage Error (%)</b>
<b>Biosoft versus actual measurement</b>	43.610
<b>Original Model</b>	34.780
<b>Knowledge Distillation-Based Model</b>	34.361
<b>Uncertainty-Aware Knowledge Distillation Based Model</b>	33.859
<b>RandAugment with Uncertainty-Aware Knowledge Distillation Based Model</b>	31.313

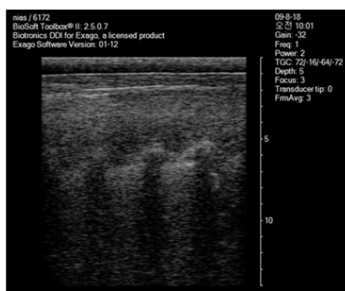
390

ACCEPTED

391 **Figure 1.** Examples of B-mode ultrasound frames at low (A), mid (B), and high (C) IMF; numbers indicate  
392 reference IMF (%)



(A) IMF : 0.9



(B) IMF : 3.576

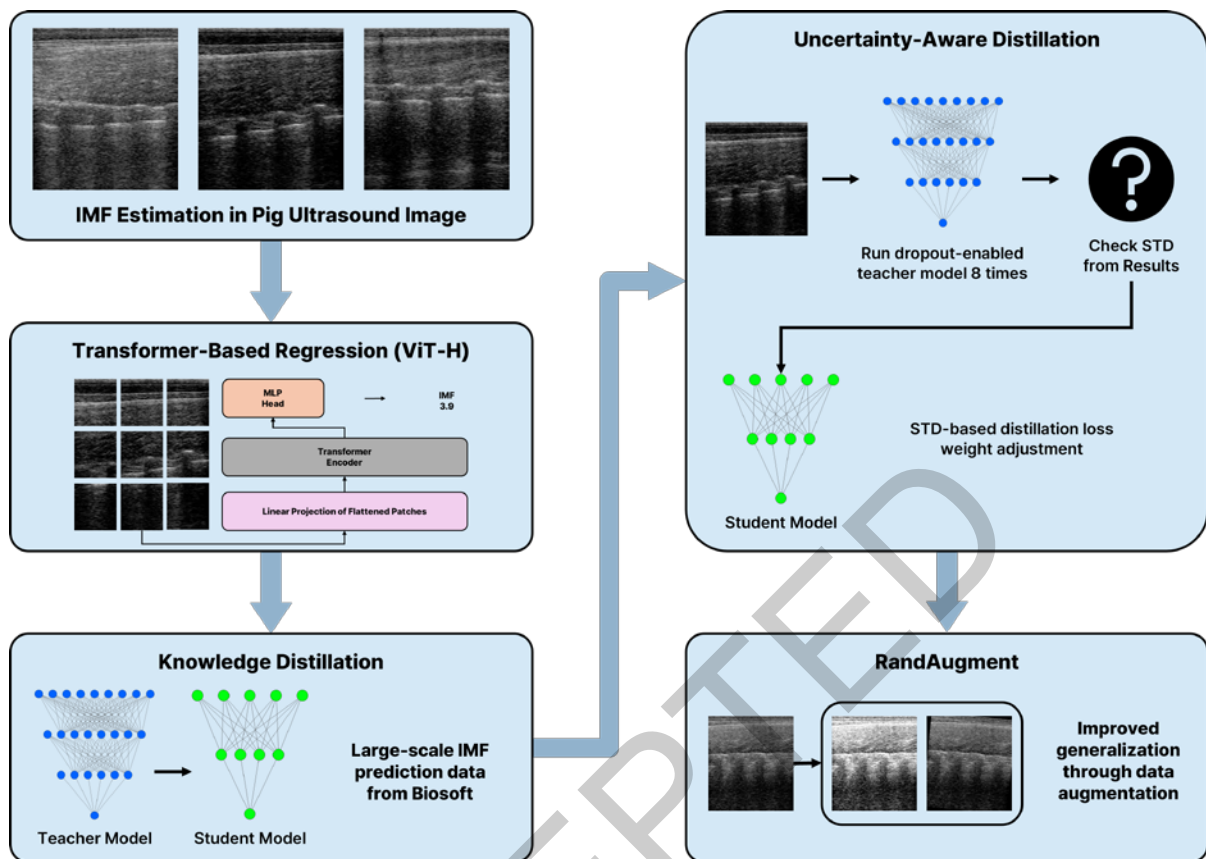


(C) IMF : 6.56

393

ACCEPTED

394 **Figure 2.** Flowchart of the proposed methodology for intramuscular fat estimation



395